JOURNAL OF VIROLOGY, Dec. 2006, p. 11467–11474 Vol. 80, No. 23
0022-538X/06/$08.00+0 doi:10.1128/JVI.01125-06

Crystal Structure of the West Nile Virus Envelope Glycoprotein▽

Grant E. Nybakken,[1] Christopher A. Nelson,[1] Beverly R. Chen,[1] Michael S. Diamond,[1,2,3] and Daved H. Fremont[1,4]*

Departments of Pathology and Immunology,[1] Medicine,[2] Molecular Microbiology,[3] and Biochemistry and Molecular Biophysics,[4] Washington University School of Medicine, St. Louis, Missouri 63110

Received 1 June 2006/Accepted 1 September 2006

The envelope glycoprotein (E) of West Nile virus (WNV) undergoes a conformational rearrangement triggered by low pH that results in a class II fusion event required for viral entry. Herein we present the 3.0-Å crystal structure of the ectodomain of WNV E, which reveals insights into the flavivirus life cycle. We found that WNV E adopts a three-domain architecture that is shared by the E proteins from dengue and tick-borne encephalitis viruses and forms a rod-shaped configuration similar to that observed in immature flavivirus particles. Interestingly, the single N-linked glycosylation site on WNV E is displaced by a novel α-helix, which could potentially alter lectin-mediated attachment. The localization of histidines within the hinge regions of E implicates these residues in pH-induced conformational transitions. Most strikingly, the WNV E ectodomain crystallized as a monomer, in contrast to other flavivirus E proteins, which have crystallized as antiparallel dimers. WNV E assembles in a crystalline lattice of perpendicular molecules, with the fusion loop of one E protein buried in a hydrophobic pocket at the DI-DIII interface of another. Dimeric E proteins pack their fusion loops into analogous pockets at the dimer interface. We speculate that E proteins could pivot around the fusion loop-pocket junction, allowing virion conformational transitions while minimizing fusion loop exposure.

West Nile virus (WNV), a member of the *Flavivirus* genus, is closely related to several arthropod-borne human pathogens, including *Japanese encephalitis virus*, *St. Louis encephalitis virus*, *Yellow fever virus*, *Dengue virus* (DENV), and *Tick-borne encephalitis virus* (TBEV). Endemic to parts of Africa, Asia, Europe, and the Middle East, WNV has recently spread to the Western Hemisphere (38). The virus cycles enzootically between birds and mosquitoes but can infect mammals, including humans. Most human infections are asymptomatic or mild, but in a small subset of individuals the infection develops into a severe neuroinvasive disease (18). Treatment for WNV infection is supportive, as there is currently no vaccine or specific therapy for use in humans (15).

The WNV genome encodes 10 proteins, including three structural (capsid, premembrane [prM], and envelope [E]) and seven nonstructural (NS1, NS2A, NS2B, NS3, NS4A, NS4B, and NS5) proteins. These are translated as a single polypeptide, which is subsequently cleaved by viral and cellular proteases (6). The initial step toward virion generation occurs when the 11-kb positive-strand RNA genome, in complex with capsid protein, buds through the endoplasmic reticulum membrane. A lipid envelope coats the nascent flavivirus particles and contains 180 molecules each of E and prM organized into 60 asymmetric trimeric spikes consisting of prM-E heterodimers (45, 46). At the apices of the spikes, prM caps the fusion loop of E (34), presumably to prevent premature fusion as the virus passes through the acidic secretory pathway (19). A furin-catalyzed membrane-proximal cleavage releases the N-terminal prepeptide from prM (39, 44), initiating the transition from immature to mature virion.

Formation of the mature virion requires structural rearrangement of the E proteins from trimeric prM-E heterodimers into homodimeric rafts that smoothly cover the lipid membrane with quasi-icosahedral symmetry (22, 28). The smooth, 500-Å-diameter surface of the mature flavivirus differs from those of many other viruses (e.g., influenza virus, human immunodeficiency virus, and alphaviruses), as it lacks spikes or protrusions. Although the structure of M remains unknown, structures for mature E as a soluble ectodomain from TBEV (33) and DENV have been determined (25, 27, 46). Each displays the same three-domain architecture. The central β-barrel consisting of eight strands defines domain I (DI), an elongated domain containing the 13-residue fusion loop at one end defines domain II (DII) (1), and the opposite end adopts an immunoglobulin (Ig)-like fold and is referred to as domain III (DIII).

The relative orientations between the three domains vary in different E structures and change during the life cycle of the virus (46). In the structures of the mature form, the hinge between DI and DII is the most variable, with the angle DII adopts ranging across ~20° (46), whereas the DI-to-DIII hinge appears to be more consistent. The postfusion structures of TBEV E and DENV type 2 (DENV-2) E reveal additional domain movements that are likely necessary for virus fusion, including the rotation and movement of DIII 33 to 36 Å toward the fusion loop (5, 26).

To understand the structural basis for the distinct tropism and pathogenesis of WNV compared to those of DENV and TBEV, we determined the X-ray crystal structure of the WNV E ectodomain. Interestingly, WNV E crystallizes as a monomer with domain orientations resembling those of E in the immature particle. We propose that our structure illus-

* Corresponding author. Mailing address: Washington University School of Medicine, Department of Pathology & Immunology, Campus Box 8118, 660 South Euclid Avenue, St. Louis, MO 63110-1093. Phone: (314) 747-6547. Fax: (314) 362-8888. E-mail: fremont@wustl.edu.

▽ Published ahead of print on 20 September 2006.

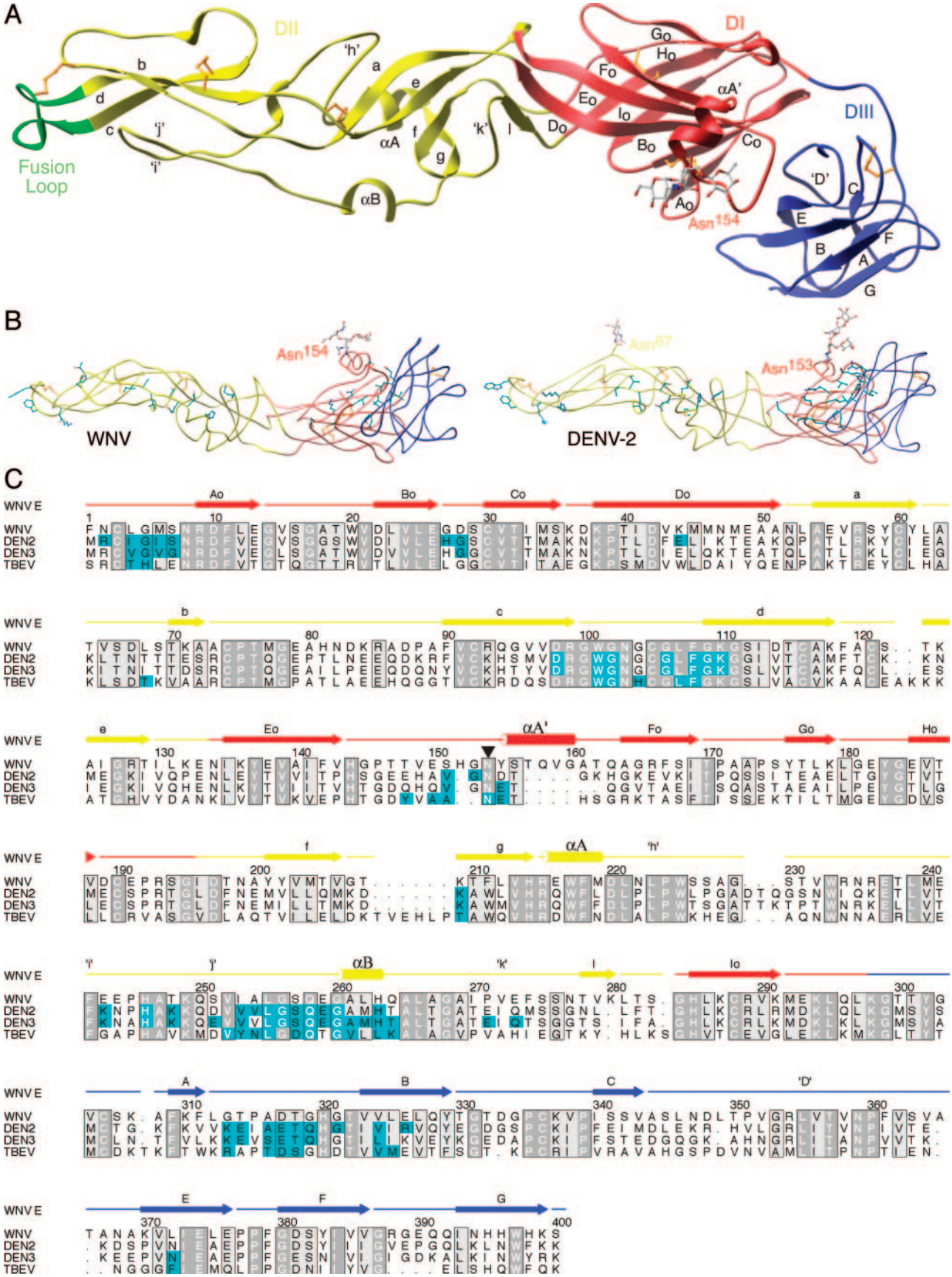
A
DII
DI
DIII
Fusion Loop
B
WNV
DENV-2
Asn154
Asn67
Asn153
C
WNV E
WNV
DEN2
DEN3
TBEV

trates features of a conformational intermediate for flavivirus E proteins.

MATERIALS AND METHODS

Expression and purification of WNV E. A cDNA encoding the ectodomain of WNV E (residues 1 to 401) from the New York 1999 strain was cloned into a baculovirus shuttle vector (pFastBac-1; Invitrogen) for expression in Hi-5 insect cells. The endogenous signal sequence (last 15 amino acids of prM) and a six-His tag were added at the N and C termini, respectively, to facilitate secretion and purification. Hi-5 cells were infected with recombinant baculovirus at a density of 2×10^6 cells per ml. The volume was doubled with ExCell 405 serum-free medium, and after 24 h, β-hydroxyecdysone was added to the culture. At 72 h postinfection, the supernatants were harvested and concentrated on a Centramate tangential-flow concentration system with a 30-kDa-cutoff membrane (Pall Life Sciences, Ann Arbor, MI). Once concentrated, the buffer was exchanged with 50 mM NaH_2PO_4, 50 mM sodium citrate (pH 8.0), 300 mM NaCl, and 0.01% NaN_3. Soluble WNV E was then captured on Ni-nitrilotriacetic acid Superflow beads (QIAGEN, Valencia, CA), washed, and eluted with binding buffer containing 250 mM imidazole (pH 8.0). The eluate was concentrated and purified further by size-exclusion chromatography, using a Superdex 200 16/60 column (GE Healthcare, Piscataway, NJ) with 20 mM HEPES (pH 7.4), 150 mM NaCl, and 0.01% sodium azide. DENV-2 E (residues 1 to 409; strain 16681) was prepared similarly, except it was buffer exchanged into 20 mM Tris (pH 8.5) and 0.01% NaN_3. DENV-2 E was recovered using MonoQ (GE Healthcare, Piscataway, NJ) fast-performance liquid chromatography and eluted using a gradient of NaCl in the same buffer.

Crystallization and data collection. Soluble WNV E was crystallized in hanging drops by vapor diffusion at 20°C. The drops contained a mixture of 0.5 μl of protein at 7 mg/ml in 20 mM HEPES (pH 7.4), 150 mM NaCl, and 0.01% NaN_3 and 0.5 μl of 11% polyethylene glycol 8000 (PEG 8000)–100 mM Tris (pH 8.4) (the precipitant solution). Crystals were cryoprotected with precipitant solution containing 30% ethylene glycol and rapidly cooled in nitrogen at 100 K. The data set was collected at Advanced Photon Source beamline BM 14 at a wavelength of 0.90 Å, using a charge-coupled device detector. Data were processed, scaled, and merged with Denzo and Scalepack (31). WNV E belongs to the $P4_12_12$ space group, with unit cell dimensions of $a = b = 89.6$ Å and $c = 154.0$ Å and with one molecule of E in the asymmetric unit.

Structure determination and refinement. The structure of WNV E was determined by molecular replacement (9), using DI and DII of DENV-2 (PDB accession no. 1OKE) and DIII from the E16 Fab-WNV DIII complex (1ZTX) as search models. Following rigid body refinement within CNS (7), model building into electron density maps was carried out in O (20), and atomic refinement was performed in CNS (7). The final R_{cryst} and R_{free} were 26.1% and 30.7%, respectively. The R values are similar to those seen for previously determined flavivirus E structures (25, 27, 33, 46). The final model contains 400 amino acids, 3 sugar molecules (2 *N*-acetyl-D-glucosamine moieties and 1 α-L-fucose moiety), and 28 water molecules.

Solution studies. Purified WNV (~1 mg) and DENV-2 (~90 μg) E proteins produced in insect cells were injected onto a Superdex 200 16/60 column (GE Healthcare, Piscataway, NJ) at 4°C. The column was calibrated using six proteins, with molecular masses of 25, 43, 67, 158, 223, and 442 kDa (GE Healthcare, Piscataway, NJ). Dynamic light scattering was performed on WNV E after passage through a 0.02-μm membrane filter (Anodisc 13; Whatman) into a 12-μl sample cuvette at 20°C at a sample concentration of 4 mg/ml in a buffer containing 20 mM HEPES (pH 7.4) and 150 mM NaCl. The experiment was performed on a DynaPro MSX molecular sizing instrument (Protein Solutions), and the data were analyzed with the Dynamics software package (V6.2).

Protein structure accession number. The coordinates for WNV E have been deposited in the RCSB Protein Data Bank (accession code 2HG0).

RESULTS

Structure of West Nile virus E protein. Recombinant, soluble E lacking the C-terminal cytoplasmic, transmembrane, and membrane-proximal 100 amino acids was produced in insect cells. WNV E crystallized in space group $P4_12_12$, with one molecule per asymmetric unit. Phasing was determined by molecular replacement using DIII of WNV E (PDB accession code 1ZTX) and DI and DII of DENV-2 E (1OKE). The structure was built and refined at a resolution of 3.0 Å to generate a final model (Fig. 1A) that includes residues 1 to 400 of E, with an R_{cryst} of 26.1% and an R_{free} of 30.7% (Table 1).

WNV E has a three-domain structure similar to that of TBEV, DENV-2, and DENV-3 (37 to 44% sequence identity and a root mean square deviation [RMSD] for Cα atoms of 2.7 to 3.5 Å). Domain I is an eight-stranded β-barrel in the center portion of the protein and is comprised of 127 amino acids (residues 1 to 51, 134 to 195, and 284 to 297) (Fig. 1A). DII, which is responsible for generating the majority of contacts in the DENV and TBEV dimers, consists of 170 residues inserted into DI (residues 52 to 133 and 196 to 283). The distal end of DII contains the putative fusion loop (residues 98 to 110), a conserved glycine-rich, hydrophobic sequence that appears necessary for flaviviral fusion (34). DIII is an Ig-like domain with seven β-strands and is similar in structure to DIII bound to the E16 Fab (29) (backbone RMSD, 0.9 Å; RMSD for all atoms, 1.5 Å) but distinct from the previously published nuclear magnetic resonance structure (43) (backbone RMSD, 2.3 Å; RMSD for all atoms, 3.8 Å). Comparing the structure of DIII in the context of the full ectodomain with the structure in complex with E16, the most significant difference between these structures lies in the DI-DIII linker regions. In the ectodomain, Tyr^{302} is tucked down alongside DIII, as in DENV and TBEV, not pointed toward the exterior of the virus as in the E16 complex (29).

Relative domain orientations. The structure of WNV E highlights the variability of domain orientations among the E proteins from WNV, DENV, and TBEV (Fig. 2). Previous crystallographic analyses of DENV and TBEV E proteins revealed a continuum of conformations at the DI-DII hinge in E (46). WNV E appears distinct from the other E structures, with a nearly 8° rotation at the DI-DII hinge region from the most similar mature crystal structure of DENV-3 E (1UZG). When the WNV E monomer is superimposed onto each DIII of the DENV-2 E dimer, this rotation results in splaying of DII from the dimer partner and the loss of numerous dimer contacts. WNV E is more similar in conformation to the immature virus E (1P58) revealed by cryo-electron microscopy (cryo-EM) (<5° rotation) than to the mature virus E (1TGE) (15° rotation) (Fig. 2).

FIG. 1. Structure of WNV E protein. (A) DI (red), DII (yellow), and DIII (blue) of monomeric E adopt a topology typical of E proteins from other flaviviruses. The fusion loop (residues 98 to 110) is highlighted in green at the tip of DII. The carbohydrate on Asn^{154}, colored according to atomicity, of DI protrudes next to a novel α-helix. Disulfide bonds are shown in gold. (B) (Left) Tube representation of WNV E, with potential dimer contacts shown in cyan. (Right) Tube representation of DENV-2 E (1OAN), with known dimer contacts shown in cyan. (C) Structural alignment of E structures from WNV, DENV-2, DENV-3, and TBEV. Contact residues within 4.0 Å of a dimer mate are colored cyan. Conservation and similarity are depicted in dark and light gray, respectively. Note the high degree of conservation among the dimerization residues. The glycosylation site is marked with an inverted triangle.

TABLE 1. Summary of data collection and refinement for WNV E

Parameter	Value or description
Data collection[a]	
Space group	$P4_12_12$
Unit cell dimensions (Å)	$a = 89.6$, $b = 89.6$, $c = 154.0$
Wavelength (Å)	0.90
X-ray source	Advanced Photon Source BM 14
Resolution(Å [range]) (outer shell range)	20–3.0 (3.19–3.00)
Total no. of observations/no. of unique observations	56,954/12,820
Completeness (%)	98.3 (99.5)
R_{sym} (%)	5.6 (42.6)
I/σ	17.7 (2.28)
Refinement statistics[b]	
Resolution (Å [range]) (outer shell range)	20–3.0 (3.19–3.00)
Reflections (R_{work}/R_{free})	11,509/607
No. of protein atoms/no. of solvent atoms/no. of heterogen atoms	3,031/25/38
R_{work} overall (outer shell) (%)	26.1 (35.9)
R_{free} overall (outer shell) (%)	30.7 (33.8)
RMSD for bond lengths (Å)/RMSD for angles (°)	0.007/1.6
RMSD for dihedral angles (°)/RMSD for improper angles (°)	24.9/0.82
Ramachandran plot parameters	
Most favored/additional (%)	76.5/23.3
Generous/disallowed (%)	0.3/0.0
Average B value	91.8
Estimated coordinate error (Å)	0.47

[a] Values as defined in SCALEPACK (31).
[b] Values as defined in CNS (7).

Oligomeric state of WNV E. Application of the tetragonal crystal symmetry operators did not create the dimer packing anticipated by previous flavivirus structures (25, 27, 33, 46), even though WNV E crystallized under similar conditions to those for DENV-2 E (11% PEG 8000, 1 M sodium formate, 20% glycerol, and 0.1 M HEPES [pH 8.0]) (25) and TBEV E (~15% PEG 4000, 0.1 M Tris-HCl [pH 8.5], 0.2 M lithium sulfate) (33). To form the tetragonal crystal lattice, there are three areas connecting symmetry-related E proteins (fusion loop-fusion loop pocket, DI-DI, and DIII-DI). These contacts display significantly less buried surface area than most physiological protein-protein interactions (250, 380, and 500 Å^2 per monomer), especially compared to the DENV-2 E protein dimer, which has 1,950 Å^2 of buried surface area per monomer (26). Size-exclusion chromatography supports the difference between the oligomeric states of WNV and DENV-2 E proteins seen in the crystal structures. Although DENV-2 E elutes with an observed molecular weight close to that of a dimer, WNV E injected at a higher concentration has a much lower apparent molecular weight (Fig. 3). Interestingly, dynamic light scattering experiments performed at a high concentration

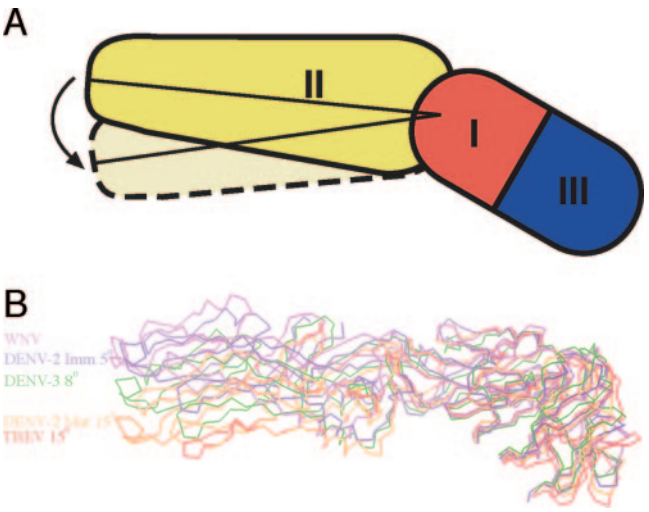

FIG. 2. WNV E has a unique interdomain orientation most similar to the structure of immature E. (A) Schematic showing the angle that was measured for each orientation of the DI-DII angle. (B) C-α traces of the WNV, DENV-3 (1UZG), and TBEV (1SVB) mature E crystal structures and the immature (1TGE) and mature (1P58) DENV-2 cryo-EM reconstructions. They overlap in DI, revealing the variability in DI-DII orientations.

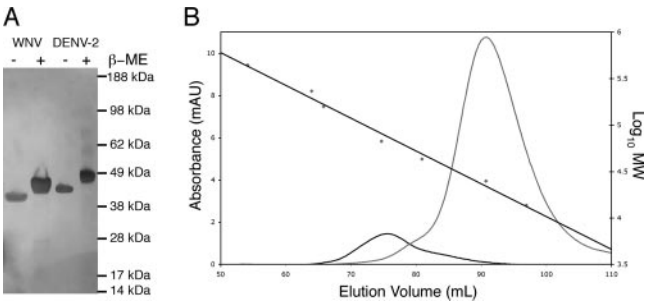

FIG. 3. DENV-2 E favors dimers more than WNV E does. (A) Silver-stained gel demonstrating similar molecular masses for DENV-2 E (calculated molecular mass, 46 kDa) and WNV E (calculated molecular mass, 44 kDa). Note that DENV-2 E has an additional glycosylation site. (B) Size-exclusion profiles for WNV E (gray) and DENV-2 E (black). The straight black line shows the calibration of the column (right axis). WNV E eluted with an observed molecular mass of 22 kDa, and DENV-2 E eluted with an observed molecular mass of 77 kDa.

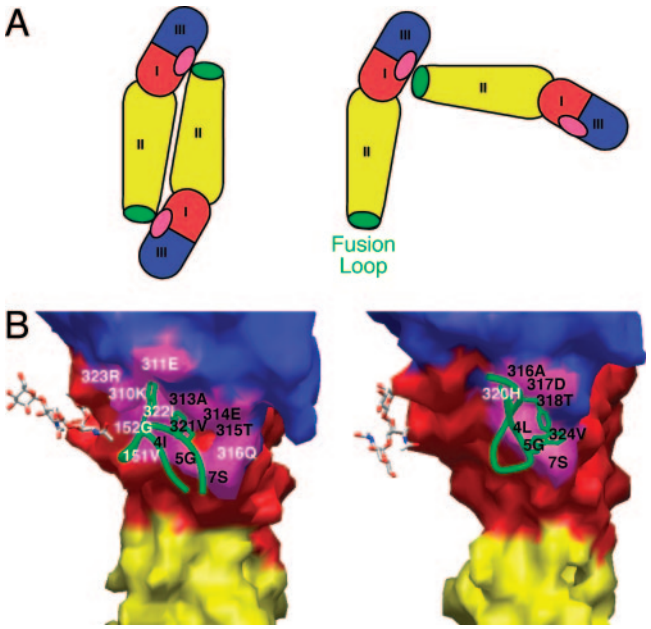

FIG. 4. The fusion loop of the WNV E monomer packs in the same pocket as that used by other flavivirus E dimers. (A) Scheme demonstrating the relative orientations of the E proteins for fusion loop packing in DENV-2 (left) and WNV (right). (B) The green worm of the fusion loop packs against similar portions of DI and DIII (magenta) in both WNV (right) and DENV-2 (left). Equivalent contact residues in both structures are labeled in black, and other contacts are shown in white.

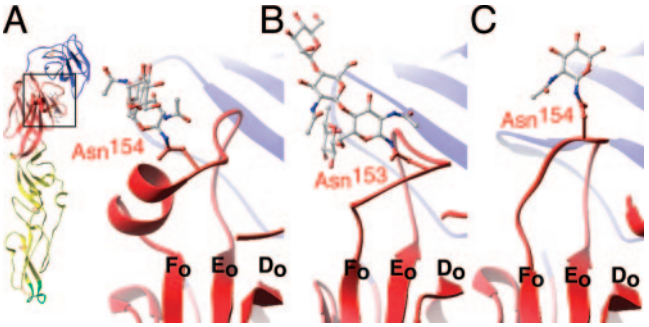

FIG. 5. Glycosylation of WNV E is shifted by a unique α-helix. (A) Ribbon figure of WNV E demonstrating a boxed area that is enlarged and shows the glycosylation (gray) of WNV E situated closely apposed to the αA′ helix. (B) Glycosylation of DENV-2 E (1OAN). (C) Glycosylation of tick-borne encephalitis virus E (1SVB).

of WNV E (~4 mg/ml) under physiologic salt and pH conditions revealed a mixture of monomers and dimers (radius, 3.4 nm; estimated molecular mass, 66 kDa). Thus, depending on the conditions and the concentration, soluble WNV E can form dimers in solution, albeit with less apparent self-affinity than that exhibited by DENV-2 E.

One possible explanation for the predominance of monomers over dimers in our studies is that WNV E has unique dimer contact residues compared to those for DENV or TBEV E. A comparison of available flavivirus E dimer structures revealed the use of similar conserved residues to generate the dimer interface (Fig. 1B and C). For WNV E, no region with extensive contacts was deleted, and high degrees of sequence identity and conservation were more than maintained (41% overall ectodomain identity, 49% identity at dimer contact residues). For example, the fusion loop residues and the equivalent contact residues along DII are all highly conserved (Fig. 1C). Examination of the structure also did not identify protruding bulges or patches along the interface regions that could create a steric hindrance. In the context of the virion, which has a high effective E protein concentration, we expect WNV E to be predominantly a dimer, as observed in the cryo-EM structure (28). The association strength may vary among different flaviviruses and could contribute to the relative stability of the virion, especially in the setting of elements that induce conformational changes (e.g., pH or furin cleavage of prM).

Fusion loop packing. Previous crystal structures showed that flavivirus E proteins form dimers by packing together in an antiparallel fashion. In these conventional dimers, the fusion loop nestles into a pocket at the DI-DIII interface created by the initial strand of DI, the E_o-F_o loop of DI, and the A-B loop of DIII (Fig. 4A). Strikingly, within the contacts of the tetragonal crystal lattice, WNV E buries its fusion loop into the very same pocket region. However, for WNV E, the contacting E proteins are oriented perpendicular to one another (Fig. 4A). Despite the radically different engagement, the fusion loop still contacts the initial strand of DI and the A-B loop of DIII, although it loses contact with the E_o-F_o loop of DI. Seven of 14 fusion loop contacts from the DENV-2 E dimer are observed in WNV E (WNV E residues 4, 5, 7, 316, 317, 318, and 324) (Fig. 4B). The buried surface areas are also similar, as fusion loops from both WNV and DENV-2 E proteins bury roughly 400 $Å^2$. The surprising similarity between the pockets suggests a propensity to bury both the fusion loop and pocket to shield them from solvent accessibility. The novel engagement seen in the WNV E crystal lattice suggests that the fusion loop pocket at the DI-DIII interface could act as a hydrophobic pivot in flavivirus conformational transitions.

N-linked glycosylation site. The WNV E protein has a single N-linked glycosylation site at Asn^{154} (Fig. 1 and 5A); this site is present in most flaviviruses but is particularly important for WNV, where it is critical for neurovirulence (3, 37). Sequence alignments revealed that the residues surrounding the Asn^{154} glycosylation are highly divergent from those of DENV and TBEV E, with a five-residue insertion surrounding the site. Interestingly, this insertion allows two turns of an α-helix, termed αA′, juxtaposed C-terminal to the glycosylation site. In contrast, the E proteins of DENV-2 and TBEV lack secondary structure in this region (Fig. 5B and C). The α-helix shifts the glycosylation site about 5 Å, to the exterior and lateral surfaces of E with respect to those of the E proteins of other flaviviruses. This movement may explain the electron density difference at the glycosylation site observed by cryo-EM for the WNV particle relative to the DENV-2 particle (28). It is interesting that the WNV E protein lacks the Asn^{67} glycosylation (Fig. 1B) that mediates the binding of DENV to DC-SIGN (32, 42) and that WNV attachment is mediated predominantly by a related lectin, DC-SIGNR (13).

Implications for low-pH transitions. Roussel et al. recently proposed for Semliki Forest virus (SFV) envelope protein E1, another class II fusion protein, that histidine residues play a

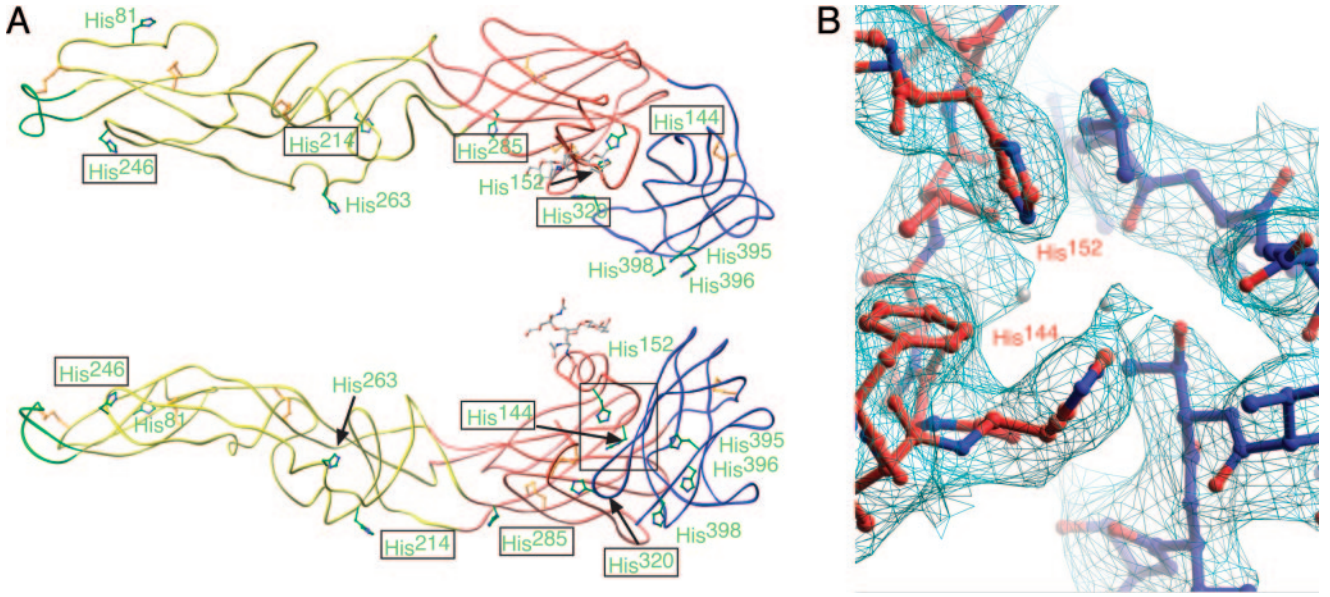

FIG. 6. Histidines are located at hinge regions of flavivirus E proteins. (A) Tube representation of WNV E, with histidine residues depicted in green, viewed from outside the virion (top) and from the perspective of a dimer partner (bottom) inside the virion. Histidines with boxed labels are structurally conserved between flavivirus structures. (B) Detailed depiction of the electron density (cyan) surrounding the histidine residues forming a base for DIII. Water molecules are depicted as gray spheres.

critical role in the conformational transition that exposes the fusion loop (35). Although generally similar, the pH of this transition varies among flaviviruses and is dependent on the lipid composition of the target membrane (40, 41). For WNV, the pH at which this change occurs has a peak around pH 6.0 (8, 14, 21), the same as the pK_a of histidine (6.0). The WNV E protein is exposed to acidic pH during receptor-mediated endocytosis.

Comparison of the available flavivirus E structures reveals that histidines are located almost exclusively at the hinge regions responsible for the low-pH transitions (Fig. 6A). Three histidines, i.e., His^{144}, His^{152}, and His^{320}, are located in the cleft between DI and DIII and provide a platform for DIII (Fig. 6B). Two other highly conserved residues, His^{214} and His^{285}, are positioned in proximity to the DI-DII hinge region and thus could be involved in movement around this axis. Residues His^{246} and His^{263} are located at the potential dimer interface; protonation of these histidines could affect the oligomeric state of E during different phases of the virus life cycle.

Another region of E that may be important in regulating fusion rearrangements lies at the DI-DII interface. Because the kl loop bound β-octyl glucoside (β-OG) in the DENV-2 E structure, it was proposed that small-molecule inhibitors that intercalate in this region could block fusion. Despite repeated attempts, we did not obtain crystals in the presence of β-OG. The kl loop of WNV adopts a conformation similar to those in other nonliganded DENV and TBEV E structures. The lack of stable insertion of β-OG in our structure could be due to differences in overall E structure or secondary to the oligomeric state (i.e., monomer) of the WNV E protein structure.

DISCUSSION

The solution of the X-ray crystal structure of West Nile virus E protein allows for a direct comparison with the E proteins of DENV and TBEV, viruses with distinct pathogeneses and tropisms. First, the glycosylation site at Asn^{154}, which is essential for the virulence of many flaviviruses, including WNV (4, 10, 17, 37), is uniquely located in our structure. An α-helical insertion C-terminal to the glycosylation site shifts the location of the sugar moiety. Carbohydrates can mediate cell attachment for flaviviruses (42), and carbohydrate spacing and type can modulate binding affinity and specificity, even between WNV and DENV (13, 16, 24). Thus, this change in the location of the carbohydrate may affect tropism. A previous study demonstrated reduced neurovirulence of WNV strains with N-linked glycosylation at Asn^{155} instead of Asn^{154} (10). In our structure, Asn^{155} projects toward the underlying β-strands. Because of its location, a carbohydrate moiety at residue 155 could destabilize this region of E.

An alignment of flavivirus E structures suggests that histidines localize to regions between domains or along the dimer interface and could participate in orchestrating pH-dependent shifts. As recently speculated for SFV, an enveloped alphavirus that also undergoes class II acid-catalyzed fusion (35), the trigger for structural transitions during the viral life cycle may be changes in the protonation of histidines, given the proximity of their pK_a to the pH at which the transitions occur. The placement of conserved histidine residues within the SFV E1 protein is analogous to the structural locations of histidine residues in flaviviruses (Fig. 6A). His^{230} in the SFV E1 protein has been shown experimentally to be required for the fusion transition (11). This histidine is structurally conserved in WNV (His^{246}) and is located at the presumptive dimer interface,

suggesting that it has a common role in the function of class II fusion proteins. Additionally, although not strictly conserved in sequence, there is a similar platform of histidine residues at the interface of DI and DIII within the SFV E1 protein. These studies highlight the similarities of class II fusion proteins and suggest a common mechanism of pH-driven structural transition.

We and others have demonstrated that DIII residues Ser^{306}, Lys^{307}, Thr^{330}, and Thr^{332} can elicit a WNV-specific neutralizing antibody response (2, 30, 36, 43). These residues cluster to a region of E that overlaps with the epitope recognized by monoclonal antibody (MAb) E16, as revealed in the crystal structure of the DIII-E16 complex (29). These residues are located in loops of the Ig-like fold that protrude from the virion and are proposed to be critical for receptor binding (33). Interestingly, all tested MAbs binding this region appear to function at a postattachment stage of infection. It is possible that these MAbs inhibit the low-pH fusion transition by restraining movement of the DI-DIII linker region, which undergoes a dramatic rearrangement during the low-pH-triggered fusion event, or by directly blocking the movement of DIII (29). The WNV E structure has a distinctly different linker residue arrangement from that found in the E16-DIII complex. In full-length WNV E, Tyr^{302} lies parallel to DIII, as seen in other unbound structures, not swung upward toward the exterior of the virion as seen when bound by E16 (29). The packing of the immature virion likely prevents adventitious fusion in the low-pH *trans*-Golgi apparatus. This packing also buries the DI-DIII linker region. A comparison of the E16 binding site with the E-E icosahedral lattice contacts in the immature virion shows overlap of the two binding sites. Thus, it appears that binding of this linker by an antibody or by another E protein may be associated with low-pH-triggered E protein conformational transitions.

A number of flavivirus neutralizing antibody epitopes localize near the fusion loop in DII. This is surprising considering that the fusion loop, paradoxically, is inaccessible in the mature virion structure (12). For example, in DENV and TBEV E dimers, the fusion loops are packed tightly into the DI-DIII interface. The WNV E protein is also assembled as a homogeneous dimer within the mature virion, as determined by cryo-EM (28). However, it remains possible that at more physiologically relevant temperatures, the WNV E protein could shift between the dimeric and monomeric configurations with intermittent or sustained exposure of the fusion loop. It appears that E proteins from different flaviviruses may have distinct dimerization affinities and may thus provide differential access to occluded binding sites by neutralizing antibodies.

In our study, although WNV E crystallized as a monomer, the E protein buried its hydrophobic fusion loop into the same pocket located at the DI-DIII interface that TBEV and DENV E proteins use to dimerize (Fig. 4). Given the multiple structural transitions in the flavivirus life cycle, it is not surprising that assembly, maturation, fusion, or some other E conformational transition may progress through monomeric intermediates. Our crystal structure of WNV E may represent one such intermediate species.

In summary, this structural analysis of the WNV E protein highlights regions of E which are critical for conformational transitions, including the DI-DIII linker, conserved histidine residues found in hinge regions, and the fusion loop. Evidence is building that conformational transitions in the life cycle of a flavivirus could be targets for inhibition by antibodies (29), small-molecule inhibitors (25), or portions of the E protein itself (23). Our investigations point to additional regions of the E protein that may be amenable to blockade. For example, the DI-DIII linker appears to be important in the fusion transition and in the transition from immature to mature viral particles. The fusion loop-pocket likely contributes to the stability of the dimer; therefore, targeting it may increase the availability of a neutralizing antibody epitope. Collectively, these and other structural studies are beginning to provide a clearer view of the conformational transitions involved in the flavivirus life cycle.

ACKNOWLEDGMENTS

We thank Phoebe Arnold for critical comments on the manuscript.

This work was supported by grants from the NIH (AI061373 to M.S.D.) and the Pediatric Dengue Vaccine Initiative (M.S.D. and D.H.F.). G.E.N. was supported by NIH Medical Scientist Training Program grant T32 GM07200 and NIH Molecular Biophysics training grant T32 GM008492. Use of the Advanced Photon Source was supported by the U.S. Department of Energy, Basic Energy Sciences, Office of Science, under contract no. W-31-109-Eng-38. Use of BioCARS Sector 14 was supported by the National Institutes of Health, National Center for Research Resources, under grant number RR07707.

REFERENCES

1. **Allison, S. L., J. Schalich, K. Stiasny, C. W. Mandl, and F. X. Heinz.** 2001. Mutational evidence for an internal fusion peptide in flavivirus envelope protein E. J. Virol. **75:**4268–4275.
2. **Beasley, D. W., and A. D. Barrett.** 2002. Identification of neutralizing epitopes within structural domain III of the West Nile virus envelope protein. J. Virol. **76:**13097–13100.
3. **Beasley, D. W., C. T. Davis, J. Estrada-Franco, R. Navarro-Lopez, A. Campomanes-Cortes, R. B. Tesh, S. C. Weaver, and A. D. Barrett.** 2004. Genome sequence and attenuating mutations in West Nile virus isolate from Mexico. Emerg. Infect. Dis. **10:**2221–2224.
4. **Beasley, D. W., M. C. Whiteman, S. Zhang, C. Y. Huang, B. S. Schneider, D. R. Smith, G. D. Gromowski, S. Higgs, R. M. Kinney, and A. D. Barrett.** 2005. Envelope protein glycosylation status influences mouse neuroinvasion phenotype of genetic lineage 1 West Nile virus strains. J. Virol. **79:**8339–8347.
5. **Bressanelli, S., K. Stiasny, S. L. Allison, E. A. Stura, S. Duquerroy, J. Lescar, F. X. Heinz, and F. A. Rey.** 2004. Structure of a flavivirus envelope glycoprotein in its low-pH-induced membrane fusion conformation. EMBO J. **23:**728–738.
6. **Brinton, M. A.** 2002. The molecular biology of West Nile virus: a new invader of the western hemisphere. Annu. Rev. Microbiol. **56:**371–402.
7. **Brunger, A. T., P. D. Adams, G. M. Clore, W. L. DeLano, P. Gros, R. W. Grosse-Kunstleve, J. S. Jiang, J. Kuszewski, M. Nilges, N. S. Pannu, R. J. Read, L. M. Rice, T. Simonson, and G. L. Warren.** 1998. Crystallography & NMR system: a new software suite for macromolecular structure determination. Acta Crystallogr. D **54:**905–921.
8. **Cammack, N., and E. A. Gould.** 1985. Conditions for haemolysis by flaviviruses and characterization of the haemolysin. J. Gen. Virol. **66:**2291–2296.
9. **CCP4.** 1994. The CCP4 suite: programs for protein crystallography. Acta Crystallogr. D **50:**760–763.
10. **Chambers, T. J., M. Halevy, A. Nestorowicz, C. M. Rice, and S. Lustig.** 1998. West Nile virus envelope proteins: nucleotide sequence analysis of strains differing in mouse neuroinvasiveness. J. Gen. Virol. **79:**2375–2380.
11. **Chanel-Vos, C., and M. Kielian.** 2004. A conserved histidine in the ij loop of the Semliki Forest virus E1 protein plays an important role in membrane fusion. J. Virol. **78:**13543–13552.
12. **Crill, W. D., and G. J. Chang.** 2004. Localization and characterization of flavivirus envelope glycoprotein cross-reactive epitopes. J. Virol. **78:**13975–13986.
13. **Davis, C. W., H. Y. Nguyen, S. L. Hanna, M. D. Sanchez, R. W. Doms, and T. C. Pierson.** 2006. West Nile virus discriminates between DC-SIGN and DC-SIGNR for cellular attachment and infection. J. Virol. **80:**1290–1301.
14. **Gollins, S. W., and J. S. Porterfield.** 1986. pH-dependent fusion between the flavivirus West Nile and liposomal model membranes. J. Gen. Virol. **67:**157–166.
15. **Granwehr, B. P., K. M. Lillibridge, S. Higgs, P. W. Mason, J. F. Aronson,**

G. A. Campbell, and A. D. Barrett. 2004. West Nile virus: where are we now? Lancet Infect. Dis. **4:**547–556.
16. **Guo, Y., H. Feinberg, E. Conroy, D. A. Mitchell, R. Alvarez, O. Blixt, M. E. Taylor, W. I. Weis, and K. Drickamer.** 2004. Structural basis for distinct ligand-binding and targeting properties of the receptors DC-SIGN and DC-SIGNR. Nat. Struct. Mol. Biol. **11:**591–598.
17. **Hanna, S. L., T. C. Pierson, M. D. Sanchez, A. A. Ahmed, M. M. Murtadha, and R. W. Doms.** 2005. N-linked glycosylation of West Nile virus envelope proteins influences particle assembly and infectivity. J. Virol. **79:**13262–13274.
18. **Hayes, E. B., and D. J. Gubler.** 2006. West Nile virus: epidemiology and clinical features of an emerging epidemic in the United States. Annu. Rev. Med. **57:**181–194.
19. **Heinz, F., K. Stiasny, G. Puschner-Auer, H. Holzmann, S. Allison, C. Mandl, and C. Kunz.** 1994. Structural changes and functional control of the tick-borne encephalitis virus glycoprotein E by the heterodimeric association with the protein prM. Virology **198:**109–117.
20. **Jones, T. A., J. Y. Zou, S. W. Cowan, and Kjeldgaard.** 1991. Improved methods for binding protein models in electron density maps and the location of errors in these models. Acta Crystallogr. A **47:**110–119.
21. **Kimura, T., and A. Ohyama.** 1988. Association between the pH-dependent conformational change of West Nile flavivirus E protein and virus-mediated membrane fusion. J. Gen. Virol. **69:**1247–1254.
22. **Kuhn, R. J., W. Zhang, M. G. Rossmann, S. V. Pletnev, J. Corver, E. Lenches, C. T. Jones, S. Mukhopadhyay, P. R. Chipman, E. G. Strauss, T. S. Baker, and J. H. Strauss.** 2002. Structure of dengue virus: implications for flavivirus organization, maturation, and fusion. Cell **108:**717–725.
23. **Liao, M., and M. Kielian.** 2005. Domain III from class II fusion proteins functions as a dominant-negative inhibitor of virus membrane fusion. J. Cell Biol. **171:**111–120.
24. **McGreal, E. P., J. L. Miller, and S. Gordon.** 2005. Ligand recognition by antigen-presenting cell C-type lectin receptors. Curr. Opin. Immunol. **17:**18–24.
25. **Modis, Y., S. Ogata, D. Clements, and S. C. Harrison.** 2003. A ligand-binding pocket in the dengue virus envelope glycoprotein. Proc. Natl. Acad. Sci. USA **100:**6986–6991.
26. **Modis, Y., S. Ogata, D. Clements, and S. C. Harrison.** 2004. Structure of the dengue virus envelope protein after membrane fusion. Nature **427:**313–319.
27. **Modis, Y., S. Ogata, D. Clements, and S. C. Harrison.** 2005. Variable surface epitopes in the crystal structure of dengue virus type 3 envelope glycoprotein. J. Virol. **79:**1223–1231.
28. **Mukhopadhyay, S., B. S. Kim, P. R. Chipman, M. G. Rossmann, and R. J. Kuhn.** 2003. Structure of West Nile virus. Science **302:**248.
29. **Nybakken, G. E., T. Oliphant, S. Johnson, S. Burke, M. S. Diamond, and D. H. Fremont.** 2005. Structural basis of West Nile virus neutralization by a therapeutic antibody. Nature **437:**764–769.
30. **Oliphant, T., M. Engle, G. E. Nybakken, C. Doane, S. Johnson, L. Huang, S. Gorlatov, E. Mehlhop, A. Marri, K. M. Chung, G. D. Ebel, L. D. Kramer, D. H. Fremont, and M. S. Diamond.** 2005. Development of a humanized monoclonal antibody with therapeutic potential against West Nile virus. Nat. Med. **11:**522–530.
31. **Otwinowski, Z., and W. Minor.** 1997. Processing of X-ray diffraction data collected in oscillation mode. Methods Enzymol. **276:**307–344.
32. **Pokidysheva, E., Y. Zhang, A. J. Battisti, C. M. Bator-Kelly, P. R. Chipman, C. Xiao, G. G. Gregorio, W. A. Hendrickson, R. J. Kuhn, and M. G. Rossmann.** 2006. Cryo-EM reconstruction of dengue virus in complex with the carbohydrate recognition domain of DC-SIGN. Cell **124:**485–493.
33. **Rey, F. A., F. X. Heinz, C. Mandl, C. Kunz, and S. C. Harrison.** 1995. The envelope glycoprotein from tick-borne encephalitis virus at 2 A resolution. Nature **375:**291–298.
34. **Roehrig, J. T., A. J. Johnson, A. R. Hunt, R. A. Bolin, and M. C. Chu.** 1990. Antibodies to dengue 2 virus E-glycoprotein synthetic peptides identify antigenic conformation. Virology **177:**668–675.
35. **Roussel, A., J. Lescar, M. C. Vaney, G. Wengler, G. Wengler, and F. A. Rey.** 2006. Structure and interactions at the viral surface of the envelope protein E1 of Semliki Forest virus. Structure **14:**75–86.
36. **Sanchez, M. D., T. C. Pierson, D. McAllister, S. L. Hanna, B. A. Puffer, L. E. Valentine, M. M. Murtadha, J. A. Hoxie, and R. W. Doms.** 2005. Characterization of neutralizing antibodies to West Nile virus. Virology **336:**70–82.
37. **Shirato, K., H. Miyoshi, A. Goto, Y. Ako, T. Ueki, H. Kariwa, and I. Takashima.** 2004. Viral envelope protein glycosylation is a molecular determinant of the neuroinvasiveness of the New York strain of West Nile virus. J. Gen. Virol. **85:**3637–3645.
38. **Solomon, T., and M. Mallewa.** 2001. Dengue and other emerging flaviviruses. J. Infect. **42:**104–115.
39. **Stadler, K., S. L. Allison, J. Schalich, and F. X. Heinz.** 1997. Proteolytic activation of tick-borne encephalitis virus by furin. J. Virol. **71:**8475–8481.
40. **Stiasny, K., and F. X. Heinz.** 2004. Effect of membrane curvature-modifying lipids on membrane fusion by tick-borne encephalitis virus. J. Virol. **78:**8536–8542.
41. **Stiasny, K., C. Koessl, and F. X. Heinz.** 2003. Involvement of lipids in different steps of the flavivirus fusion mechanism. J. Virol. **77:**7856–7862.
42. **Tassaneetrithep, B., T. H. Burgess, A. Granelli-Piperno, C. Trumpfheller, J. Finke, W. Sun, M. A. Eller, K. Pattanapanyasat, S. Sarasombath, D. L. Birx, R. M. Steinman, S. Schlesinger, and M. A. Marovich.** 2003. DC-SIGN (CD209) mediates dengue virus infection of human dendritic cells. J. Exp. Med. **197:**823–829.
43. **Volk, D. E., D. W. Beasley, D. A. Kallick, M. R. Holbrook, A. D. Barrett, and D. G. Gorenstein.** 2004. Solution structure and antibody binding studies of the envelope protein domain III from the New York strain of West Nile virus. J. Biol. Chem. **279:**38755–38761.
44. **Wengler, G., and G. Wengler.** 1989. Cell-associated West Nile flavivirus is covered with E+pre-M protein heterodimers which are destroyed and reorganized by proteolytic cleavage during virus release. J. Virol. **63:**2521–2526.
45. **Zhang, Y., J. Corver, P. R. Chipman, W. Zhang, S. V. Pletnev, D. Sedlak, T. S. Baker, J. H. Strauss, R. J. Kuhn, and M. G. Rossmann.** 2003. Structures of immature flavivirus particles. EMBO J. **22:**2604–2613.
46. **Zhang, Y., W. Zhang, S. Ogata, D. Clements, J. H. Strauss, T. S. Baker, R. J. Kuhn, and M. G. Rossmann.** 2004. Conformational changes of the flavivirus E glycoprotein. Structure (Cambridge) **12:**1607–1618.